33rd Annual International Conference of the IEEE EMBS
Boston, Massachusetts USA, August 30 - September 3, 2011

Software-Based Microwave CT System Consisting of Antennas and Vector Network Analyzer

Takahiro OGAWA , *Member, IEEE*, and Michio MIYAKAWA , *Member, IEEE*

Abstract— **We have developed a software-based microwave CT (SMCT) that consists of antennas and a vector network analyzer. Regardless of the scanner type, SMCT collects the S-parameters at each measurement position in the frequency range of interest. After collecting all the S-parameters, it calculates the shortest path to obtain the projection data for CPMCT. Because of the redundant data in SMCT, the calculation of the projection is easily optimized. Therefore, the system can improve the accuracy and stability of the measurement. Furthermore, the experimental system is constructed at a reasonable cost. Hence, SMCT is useful for imaging experiments for CP-MCT and particularly for basic studies. This paper describes the software-based microwave imaging system, and experimental results show the usefulness of the system.**

I. Introduction

Biomedical microwave-imaging technologies have been developed to obtain temperature information for hyperthermia treatment of cancers. These technologies measure the distribution of temperature change in the human body [1], [2] and conduct diagnostic imaging of tumor-formation and brain-hemorrhage sites [3].In recent years, the microwave imaging of extremity soft tissues for obtaining functional-information has been extensively studied [4].

Chirp-pulse microwave computed tomography (CP-MCT) systems [1], [2], [5]–[7] determine the propagation path of a signal passing through an object using a chirp signal in the microwave band and obtain the projection data from the amplitude of the transmitted signals. These systems generally include hardware devices applicable in the microwave band such as a chirp-signal generator, a high-frequency amplifier, and a mixer. However, the image quality of the system depends on the system performance and adjustment of the hardware components. In the study of a computed tomography (CT) system using a microwave, the major task is to investigate the relationship between the characteristics of the microwave and imaging data. Therefore, it is not undesirable that the imaging results are influenced by the hardware performance. Our software-based microwave computed tomography (SMCT) system replaces the high-frequency hardware devices other than the antenna device with a vector network analyzer (VNA). The tomographic images are obtained by a numerical calculation of the measured S-parameters. The S-parameters contain the amplitudes and phases of microwaves reflected by and transmitted through the measured objects, which are treated as black boxes. Therefore, the analysis of tomographic information using S-parameters provides useful information such as phase information and amplitude information. Thus, we have developed an SMCT system that can obtain a tomographic image of the amplitude and phase change. Here, we outline the system and verify its usefulness experimentally.

Manuscript received August 27, 2010. This work was supported in part by the Grant-in-Aid for Scientific Research (B) (#22300151) by Japan Society for the Promotion of Science.

T. Ogawa is a student at Graduate School of Science and Technology, Niigata University, Niigata, 50-2181 Japan. He is the President with MEL Incorporated, Nagoya, 452-0808 Japan. (ogawa@melinc.co.jp)

M. Miyakawa is with the Institute of Science and Technology, Niigata University, Niigata 950-2181 Japan. (miyakawa@eng.niigata-u.ac.jp)

II. Method

A. Outline of principle of CP-MCT system and conventional system configuration

Figure 1 shows a schematic diagram of a prototype CP-CMT system that uses our own hardware devices. A chirp signal is emitted from Antenna A and received by Antenna B. The signal component that follows each propagation path can be divided into various signal components that propagate along different paths. We first multiply the input chirp signal by a chirp signal that is received by Antenna B and amplified. We then extract the components of a specific term from this multiplied signal. An input chirp signal whose angular frequency changes from ω_1 to ω_2 during the sweep time can be represented by

$$S_r(t) = A\sin(\omega_1 t + Kt^2/2) \quad (1)$$

$$where\ K = (\omega_2 - \omega_1)/T_s \quad (2)$$

A signal component received by Antenna B that follows a specific path P_i has a phase that lags T_i behind the input chirp signal $S_r(t)$ and an amplitude that is α_i times the input chirp signal $S_r(t)$. By multiplying this signal component by the input chirp signal $S_r(t)$ and passing the multiplied component through a low-pass filter, we obtain the following signal:

$$S_{bi}(t) = \alpha_i A^2/2\cos[KT_i t + \omega_1 T_i - KT_i^2/2] \quad (3)$$

That is, the output signal component is a sinusoidal wave with an amplitude of $\alpha_i A^2/2$ and a frequency of $KT_i/2\pi$. Thus, the total output signal $S_b(t)$ is a composite wave consisting of

output signal components with different frequencies according to the propagation path. We can divide the output signal into the signal components with different frequencies using a Fourier transform. We then choose the signal component with the largest amplitude. We can thus extract the dominant signal component from the different components, each of which propagates along a different propagation path. The dominant signal can be regarded as the signal that propagates along a straight line. By measuring the peak value of the dominant signal while changing the antenna positions, we can obtain one-dimensional projection data. The mechanism just described is the principle of the Chirp Pulse Microwave CT system(CP-MCT). CP-MCT systems determine the transmitted signal on the straight path $S_{bi}(t)$ using hardware devices.

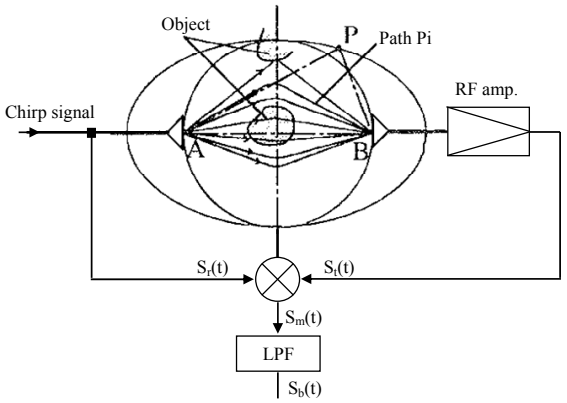

Fig. 1. Principle of CP-MCT using chirp pulse signal.

B. Software-based detection of propagation path

As shown in Fig. 1, the SMCT system replaces the hardware devices other than the antennas with a VNA and software processing. The SMCT system measures the necessary S-parameters in each rotation position by controlling a rotational scanner and the VNA. From these data, we can calculate the tomographic image. By definition, the discrete Fourier transform of the chirp signal shown in Eq. (1) can be represented as follows:

$$A_k = \frac{1}{N}\sum_{i=0}^{N-1} e^{-j\frac{2\pi k}{N}i} S_r(t_i), \quad (k = 0,1,\cdots,N-1) \tag{4}$$

where N is the number of sampling points, t_i is the ith sampling time, and k is the kth spectrum. Hereafter, we refer to this as a discrete chirp signal.

Based on the measurement principle shown diagrammatically in Fig. 1, we can divide the output signals according to propagating path by numerical calculation using the equivalent circuit shown in Fig. 2. In Fig. 2, the S-parameters are obtained by the VNA and matched with the system impedance. The discrete chirp signal given in Eq. (4) is input to the circuit. By calculating the voltage at the output end, we obtain the receiver output signal for the input discrete chirp signal. In the case where spectra up to the Mth discrete chirp signal are considered, the compound mixer output $V_0(t)$ is represented as

$$V_o(t) = \sum_{p=0}^{M}\sum_{q=0}^{M} \hat{A}_p \hat{S}_q^* e^{j|\omega_p - \omega_q|t} \tag{5}$$

where $\hat{A}_p$ is the p-th phasor of the discrete chirp signals, and $\hat{S}_q^*$ is the complex conjugate of q-th phasor of the S-parameter output signal obtained by the calculation.

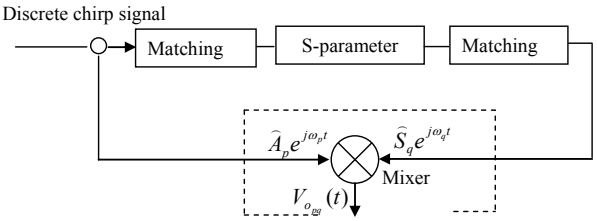

Fig. 2. Equivalent circuit of SMCT based on the principle of CP-MCT.

III. EXPERIMENTAL VERIFICATION

The hardware of the SMCT system is easily adaptable to both fan-beam and parallel-beam scanners. We conducted an imaging test using the fan-beam CT scanner as illustrated in Fig. 3. The distance between the transmitting and receiving antennas is 176 mm. The number of receiving antennas is 31, and each antenna aligns with an 8-mm pitch. The fan angle is 87.9º, and the region of measurement is a circle with a diameter of approximately 122 mm [8].

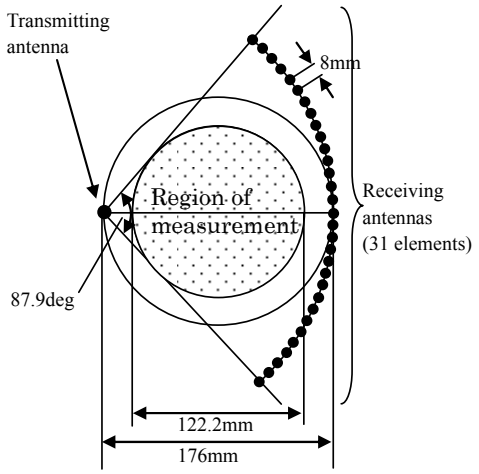

Fig. 3. Structure of the fan beam CT scanner.

A. Experiment 1

The first set of imaging objects are two phantoms of pure water, each of which is contained in a 0.5-mm-thick and 38-mm-diameter plastic container. The two objects are immersed in a saline bolus at a concentration of 0.15% and a temperature of 21.2°C. Figure 4(a) shows the arrangement of the two objects. Figure 4(b) shows the contour sinogram

obtained by calculating the amplitude components. The discrete chirp signal is swept at 1 to 2 GHz during a sweep time of T_s = 200 ns. Because the objects are located in an offset position, the contour sinogram exhibits the meander behavior associated with rotation. The reconstructed images are shown in Fig. 5. The superimposed circle indicated by a short dashed line shows the location of each object. Figure 5(a) shows the reconstructed amplitude image, and Fig. 5(b) shows the reconstructed phase image of the objects, which is smaller and clearer than the amplitude image of the objects.

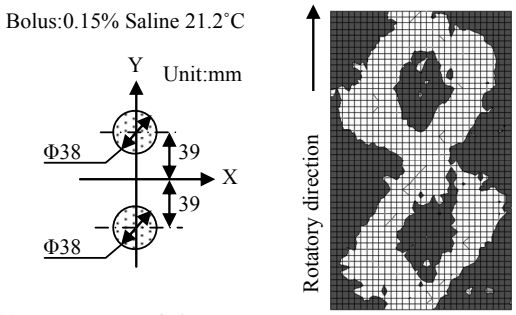

(a) Arrangement of phantoms (b) Sinogram

Fig. 4. Phantom arrangement in Experiment-1 and the sinogram .

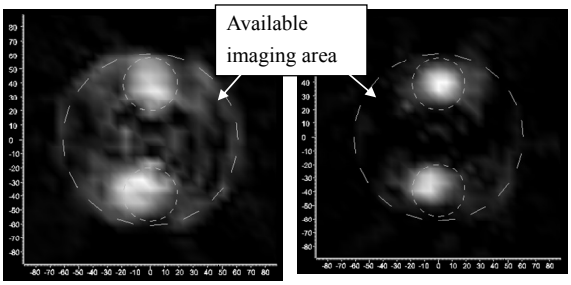

(a) Amplitude image (b) Phase image

Fig. 5. Reconstruct Images in Experiment-1.

B. *Experiment 2*

The second set of imaging objects are three phantoms of pure water, contained in plastic containers of diameter 50 mm, 25 mm, and 27 mm, respectively, and one phantom of a 0.3% salt solution, contained in a plastic container of diameter 38 mm. The four objects are immersed in a saline bolus at a concentration of 0.15% and a temperature of 22°C. Figure 6(a) shows the arrangement of the four objects. The discrete chirp signal is swept at 1 to 3 GHz during a sweep time of T_s = 200 ns. Figure 6(b) shows the contour sinogram obtained by calculating the amplitude components. The reconstructed images are shown in Fig. 7. The superimposed circle indicated by a short dashed line shows the location of each object. Figure 7(a) shows the image reconstructed by the amplitude components. The image of the 38-mm-diameter object is observed as a black area, because the concentration of the solution is higher than that of the bolus. The image of the 50-mm-diameter object is observed as a small white area. The salt concentration is reconstructed properly in these images. In other words, these images are normal. However, the images of the objects of diameter 25 mm and 27 mm are observed as black areas. That is, a white-to-black reversal phenomenon occurs in these images, although the salt concentrations of the solutions are lower than that of the bolus. This is believed to be caused by the relationship between the chirp-signal frequency and the object size; the details are now being studied. Figure 7(b) shows the reconstructed image of the phase components. In this figure, the images of the objects of diameter 25 mm and 27 mm are normal, although the white-to-black reversal phenomenon occurs in their amplitude images. To summarize the image patterns shown in Fig. 7, we can say that in the amplitude image, the images of the large objects are clear, and, in contrast, in the phase image the images of the small objects are normal with no white-to-black reversal phenomenon.

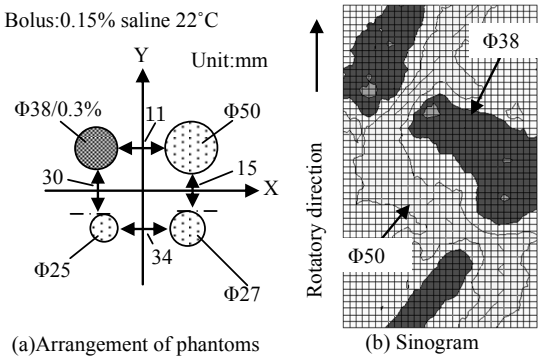

(a)Arrangement of phantoms (b) Sinogram

Fig. 6. Phantoms arrangement in Experiment-2 and the sonogram.

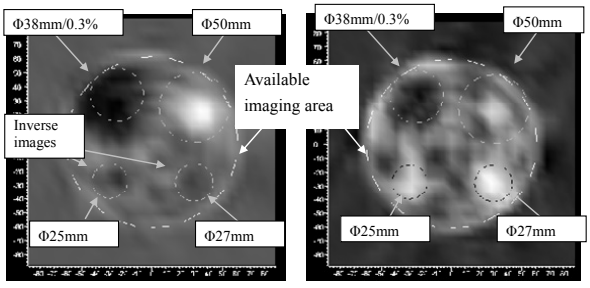

(a) Amplitude image (b) Phase image

Fig. 7. Reconstruct Images in Experiment-2.

IV. SUMMARY

We have presented a software-based chirp-pulse microwave CT scanner using only a VNA and two antennas. We conducted an imaging test and demonstrated the appropriateness of this CT algorithm. We confirmed that imaging data can be obtained from either the amplitude or the

phase components. In the reconstructed image, objects can be imaged with clarity depending on their features of object; a white-to-black reversal phenomenon sometimes occurs. We can change the chirp-signal frequency freely in the range of the measurement bandwidth after the completion of the measurement. In addition, the ability to acquire the amplitude and phase information concurrently enables us to obtain a variety of information from a single measurement. Our method has the following advantages:

1) Because the S-parameters are calculated after the completion of the measurement, we can change the frequency of the chirp signal, switch between amplitude and phase image information, or change the matching conditions after completing of the measurement.
2) When we study the relationship between microwave properties and imaging information, which is an important objective, the frequency band of the chirp signal and the bandwidth can easily be changed by replacing the VNA and antennas. The study can therefore be performed without being influenced by high-frequency techniques.
3) The necessary hardware devices in addition to the VNA are the antennas and a mechanical scanner for rotating the antennas. Therefore, the hardware cost is low, and maintenance can easily be carried out.
4) The measurements can be simulated. Therefore, various inspections can be carried out. The current challenges are to reduce the measurement time and to extend the dynamic range.

The current VNA takes one hour for the measurement and requires the concentration of the bolus to be 0.3% or less. However, when a more powerful VNA is used, a high-concentration bolus can be measured in approximately five minutes. As described above, by using a general-purpose measuring instrument and making full use of the software, we can increase the system flexibility significantly. Thus, identical experimentation environments can easily be constructed. Our software-based microwave CT system can contribute significantly to research in this field and is commercially viable.

V. Acknowledgement

The authors thanks R. Kuniyasu at Niigata university for his contribution, including measurement data. This research was partially supported by a Grant-in-Aid for Scientific Research ((B): #22300151).

References

[1] M. Miyakawa, D. Watanabe, and Y. Saito, "Imaging of the temperature change by the improved chirp radar-type microwave computed tomography," Trans. IEE Japan (in Japanese), vol. 112-C, no. 8, pp. 493-499, 1992.

[2] M. Miyakawa, "Tomographic measurement of temperature change in phantoms of the human body by chirp radar-type microwave computed tomography," Med. & Biol. Eng. and Comput., vol. 31, no. 4-S, pp. 31-36, 1993.

[3] M. Miyakawa, K. Sugawara, M. Bertero, and M. Piana, "Computational imaging of the breast- and head-models in CPMCT," Proc. PIERS 2002 in Cambridge, pp. 593, 2002.

[4] S. Semenov, J. Kellam, P. Althaussen, et al. "Microwave tomography for functional imaging of extremity soft tissues: Feasibility assessment," Phys. Med. Biol., vol. 52, pp. 5705-5719, 2007.

[5] M. Miyakawa, "An attempt of microwave imaging of the human body by the chirp rad-type microwave," Trans. IEICE (in Japanese), vol. J75-D-II, no. 8, pp. 1447-1454, 1992.

[6] M. Bertero, M. Miyakawa, P. Boccacci, F. Conte, K. Orikasa, and M. Furutani, "Image restoration in chirp pulse microwave CT (CP-MCT)," IEEE Trans. Biomedical Engineering, vol. 47, no. 5, pp. 690-699, 2000.

[7] M. Bertero, F. Conte, M. Miyakawa, and M. Piana, "Computation of the response function in chirp-pulse microwave computerized tomography," Inverse Problems, vol. 17, pp. 485-500, 2001.

[8] M. Miyakawa, T. Yokoo, N. Ishii, and M. Bertero, "Visualization of human arms and legs by CP-MCT," Proc. 38th European Microwave Conference, CD-ROM, pp. 412-415, 2008.